Fluctuations, temperature, and detailed balance in classical nucleation theory

Robert McGraw
Environmental Chemistry Division, Brookhaven National Laboratory, Upton, New York 11973

Randall A. LaViolette
Idaho National Engineering Laboratory, P.O. Box 1625, Idaho Falls, Idaho 83415

The role of temperature in classical nucleation theory is examined. It is shown that while even small clusters are assigned a temperature in the classical theory, this must be a fluctuating quantity. Stochastic simulations of cluster evaporation and growth are presented to track the temperature fluctuations in time. The relation $\langle |\delta T|^2 \rangle = kT_0^2/C_\nu$ for the mean square temperature fluctuation is confirmed, where k is the Boltzmann constant, C_ν is the cluster heat capacity, and T_0 is the bath temperature. For small capillary drops (50–100 molecules), the resulting rms temperature fluctuations of $10°$–$20°$ might be expected to have a significant effect on the nucleation rate. However, the simulations reveal a cluster temperature distribution that is centered several degrees below T_0. A theory is presented to explain this effect. To first order, which includes Gaussian fluctuations of the cluster temperature T, we find that the effective temperature for cluster evaporation is $T - h/2C_\nu$, where h is the latent heat. This temperature correction is precisely that required by detailed balance and results both in a centering of the cluster temperature distribution on T_0 and a cancellation of any significant effect of temperature fluctuations on the nucleation rate. © *1995 American Institute of Physics.*

I. INTRODUCTION

The assignment of a temperature to small systems, on the size of molecular clusters, is perhaps nowhere more explicit than in the capillarity approximation of classical nucleation theory.[1] This approximation can take on a number of corrected forms, but its essence is that a cluster embryo is modeled as a liquid drop (or solid particle) having the bulk properties of the nucleated phase. Among these is a well-defined temperature, which is generally set equal to the temperature of the surrounding vapor bath for computing cluster properties, but can be hotter than the bath at finite nucleation rates due to the release of latent heat.[2] The capillarity approximation also includes assignments for the density, heat capacity, surface tension, and evaporation rate, all in terms of the temperature of the drop. The notion of a cluster temperature is therefore well rooted in the classical theory and appears to be required, at least until development of a fully molecular treatment of nucleation based solely on cluster energy.

The role of temperature in classical nucleation theory has been examined from several directions. Studies of nonisothermal nucleation have shown that high nucleation rates require the dissipation of the latent heat of condensation, resulting in an elevation of the cluster temperature above the temperature of the bath, but the inclusion of this effect does not significantly alter the nucleation rate.[2–5] The effect of temperature fluctuations on the nucleation rate has also been examined.[6,7] These latter studies attempted to include the effect of fluctuations in cluster temperature about the temperature of the bath (T_0). The fluctuation distribution was taken to be Gaussian and centered on T_0. However, since the evaporation rate increases exponentially with temperature, it was observed that the evaporation rate, weighted by the cluster temperature distribution, exceeded the evaporation rate of the cluster at the temperature of the bath. The excess evaporation, over that required to satisfy detailed balance, resulted in the prediction of an unphysically large (26 orders of magnitude) reduction in the nucleation rate.[6] That conclusion has been tempered in more recent work.[8] The present paper builds on results from a preliminary study of temperature fluctuations in nucleation, in which the simulation model described in Sec. IV was presented.[9]

There are well-known difficulties in the assignment of temperature to small systems coupled to a heat bath[10] and considerable controversy.[11,12] Thus, when possible, the method of choice is to work within the framework of fluctuations in energy rather than temperature. However, within the framework of the capillarity approximation, it does not make a substantial difference which formulation is applied because the bulk heat capacity provides a functional relation between changes in temperature and changes in energy of the cluster embryo modeled as a liquid drop ($dE = C_\nu dT$). Consequently, the difficulties associated with the introduction of temperature fluctuations in the capillary drop model will not be resolved simply by changing to an energy description. As shown in Sec. III, a more substantial modification, in the form of a correction to the evaporation rate of small clusters, is required.

In this paper we examine the role of temperature in nucleation theory from the standpoint of fluctuations in both the cluster temperature and cluster energy. When it becomes necessary to adopt a statistical model (e.g., to evaluate the density of states of a small cluster) the capillarity approximation will be used. It is shown that if temperature fluctuations are included, care must be taken in assigning the cluster temperature when the process under consideration (e.g.,

evaporation, molecular collision) results in transfers of energy that are an appreciable fraction of the cluster energy itself. A similar situation has long been encountered in statistical descriptions of atomic nuclei in which temperature was introduced.[11,13,14] Here the emission of even one particle constitutes a relatively large loss of energy, which reduces the temperature considerably. Careful analysis reveals that the temperature determining the energy distribution of emitted particles is not the temperature of the nucleus before emission, but the temperature after emission has occurred.[14] In the following sections we adapt similar methods and obtain a similar result. We will find that to first order in size correction the fluctuations are Gaussian and centered on T_0. However, the temperature appearing in the Clapeyron equation for the cluster evaporation rate is shown to not be the temperature of the cluster before evaporation of a molecule occurs, as is usually assumed, but an average of the cluster temperatures before and after evaporation has occurred. This distinction is important when the cluster size is small.

In Sec. II we present a description of detailed balance, as it is used in classical nucleation theory, to derive the fluxes for cluster evaporation and growth. When temperature fluctuations are introduced, without correction for the effects of large fractional energy exchange, it is found that the detailed balance condition is violated; the average rate of evaporation exceeds the rate of molecular accommodation, resulting in a violation of the second law. The resolution of the problem is presented in Sec. III through the derivation of the corrected cluster evaporation rate described earlier. In Sec. IV we apply the capillarity approximation to simulations of droplet evaporation and growth. Initially we calculate the evaporation rate in the conventional manner without temperature correction. In the absence of a carrier gas it is found that the temperature distribution is shifted below the bath temperature by the precise amount required for detailed balance to hold, nonetheless inconsistencies remain. Again the problems are resolved when the corrected evaporation rate of Sec. III is used. Then it is found that the simulated fluctuation spectrum is centered on the bath temperature *and* the detailed balance condition is satisfied.

Distributions for temperature and energy fluctuations in a capillary drop are derived in the Appendix using the Einstein fluctuation formula.[15] A Carnot engine coupling between the drop and the bath is used to compute the reversible work required to shift the drop temperature from that of the bath. For small values of the reciprocal particle size, the fluctuations in both temperature and energy reduce to Gaussian form and the fluctuations in temperature are centered on the temperature of the bath. One consequence of working in the Gaussian limit of large particle size is that it becomes apparent that the fluctuation distributions are not required to be non-Gaussian for resolution of the difficulties associated with the preservation of detailed balance. Section V presents a discussion of these results.

II. THE EFFECT OF FLUCTUATIONS ON CLUSTER ENERGY AND MASS BALANCE

The evaporation rate enters into the net flux for the conversion of clusters of size g to size $g+1$, where g is the number of molecules in the cluster. The net flux takes the form

$$J(g,g+1) = \beta_1 s_g f_g - \gamma_{g+1} s_{g+1} f_{g+1}, \qquad (2.1)$$

where β_1 is the accommodation rate, per unit area of surface, for molecules of the condensable vapor, γ_{g+1} is the evaporation rate, and s_g and f_g are the surface area and number concentration, respectively, for clusters of size g. For a vapor accommodation coefficient of unity,

$$\beta_1 = (2\pi m_1 kT)^{-1/2} p_1, \qquad (2.2)$$

where m_1 and p_1 are the molecular mass and partial pressure of the vapor species at temperature T. At equilibrium the net flux vanishes to give the detailed balance condition as it appears in classical nucleation theory:

$$\beta_1 s_g n_g = \gamma_{g+1} s_{g+1} n_{g+1}, \qquad (2.3)$$

where n_g is the cluster concentration at equilibrium.

The equilibrium cluster concentrations are obtained, in the usual manner, from the reversible work required to bring about their formation from the vapor.[1] This results in a determination of the evaporation rate as

$$
\begin{aligned}
\gamma_{g+1} &= \beta_1 s_g n_g / (s_{g+1} n_{g+1}) \\
&= \beta_1 (s_g/s_{g+1}) \exp\left\{ -\ln S + \left[\frac{\sigma}{kT}(s_{g+1} - s_g) \right] \right\} \\
&= (s_g/s_{g+1})(2\pi m_1 kT)^{-1/2} p_1(\infty, T) \\
&\quad \times \exp\left[\frac{\sigma}{kT}(s_{g+1} - s_g) \right] \\
&\cong (s_g/s_{g+1})(2\pi m_1 kT)^{-1/2} p_1(\infty, T) \exp\left(\frac{2\sigma}{r_g kT} \nu_1 \right),
\end{aligned}
\qquad (2.4)
$$

where, beginning with the second equality, the capillarity approximation is used. The equilibrium vapor pressure over a flat surface is $p_1(\infty, T)$, $S = p_1/p_1(\infty, T)$ is the supersaturation ratio, and σ is the surface tension. The last equality was obtained using $s_{g+1} - s_g \cong ds_g/dg$ for a cluster modeled as a spherical drop where r_g is the g-cluster radius and ν_1 is the molecular volume of the nucleating species. The last two equalities in Eq. (2.4) show the required independence of the evaporation rate on the concentration of vapor. The last two factors in Eq. (2.4) give the Kelvin relation for the vapor pressure in equilibrium over a surface with radius of curvature r_g. Equation (2.2) shows that the condensation rate is proportional to the pressure p_1 of the surrounding vapor. Equation (2.4) shows that the evaporation rate is proportional to the vapor pressure of the drop. A more complete discussion of the thermodynamic assumptions behind the transition from Eqs. (2.1) to (2.4) is found in Ref. 16.

From the Clapeyron relation

$$\frac{d \ln p_1(\infty, T)}{dT} = \frac{h}{kT^2}, \tag{2.5}$$

where h is the bulk latent heat per molecule and we obtain from Eq. (2.4),

$$\frac{d \ln \gamma_{g+1}}{dT} = \frac{h_d}{kT^2} - \frac{1}{2T} \cong \frac{h_d}{kT^2}, \tag{2.6}$$

where h_d includes the drop curvature correction

$$h_d = h - 2\sigma \nu_1 / r_g \tag{2.7}$$

and the last equality of Eq. (2.6) follows for $kT \ll 2h_d$. [Equation (2.7) will require correction for the temperature derivative of σ if the latter is a strong function of T.] The curvature correction in Eq. (2.7) is less than 10% over the size range of the 50–300 molecule water clusters studied in the simulations. Thus we will neglect *changes* in curvature correction with small changes in g to obtain

$$\gamma_{g+1}(T) = \gamma_{g+1}^{cl} \exp\left[\frac{h_d}{k}\left(\frac{1}{T_0} - \frac{1}{T}\right)\right], \tag{2.8a}$$

where

$$\gamma_{g+1}^{cl} \equiv \gamma_{g+1}(T_0) \tag{2.8b}$$

is the evaporation rate from Eq. (2.4), evaluated at the temperature of the bath. The superscript cl emphasizes that γ_{g+1}^{cl} is the evaporation rate, per unit area of surface, for a cluster of size $g+1$ in the classical nucleation theory. Specifically, γ_{g+1}^{cl} is an approximation to γ_{g+1} of Eq. (2.3) that results after the capillarity approximation has been applied. Temperature dependence has been omitted since it is understood that γ_{g+1}^{cl} is evaluated only at the temperature of the bath. In the remainder of the paper it is shown that Eq. (2.8) correctly gives the evaporation rate for an ensemble of clusters as a function of the temperature of the bath, but should not be applied to individual clusters coupled to the bath. Henceforth, we continue to use T_0 for the temperature of the bath and use T exclusively for the temperature of a cluster coupled to the bath in the capillarity approximation. The former is a constant, since the bath is assumed large, while the latter is a fluctuating quantity.

Equation (2.8) is tested in the simulation model of Sec. IV where it is used to evaluate the evaporation rate for clusters subject to fluctuations in temperature about T_0. However, even without simulation it is evident that there are difficulties inherent in applying Eq. (2.8) to individual clusters, as opposed to an ensemble of clusters. The major problem, violation of the detailed balance condition, when fluctuations in temperature and energy of the cluster are included, will now be described.

Fluctuations in temperature and energy of a small capillary drop are described by the distribution functions developed in the Appendix. The average evaporation rate, averaged over the normalized temperature distribution $P(T)$ of Eqs. (A8) and (A9), is defined as

$$\overline{\gamma_{g+1}(T)} = \int \gamma_{g+1}(T) P(T) dT. \tag{2.9}$$

In the Appendix it is shown that the average value of the reciprocal temperature, averaged over $P(T)$, equals the reciprocal of the temperature of the bath [Eq. (A10)]. This result, together with the property that $\exp(-h_d/kT)$ is a concave function for $kT < h_d/2$, which is well satisfied over the temperature range of interest [see, also, the inequality following Eq. (2.7)], meets the requirements for Jensen's inequality[17] to hold. In the present case Jensen's inequality takes the form

$$\overline{\gamma_{g+1}(T)} \geqslant \gamma_{g+1}^{cl}. \tag{2.10}$$

For the special case that $P(T)$ is approximated by a Gaussian distribution [Eq. (A13)],

$$P(T) \cong \left(\frac{C_\nu}{2\pi kT_0^2}\right)^{1/2} \exp\left(\frac{-C_\nu(T-T_0)^2}{2kT_0^2}\right) \equiv f_0(T), \tag{2.11}$$

where C_ν is the heat capacity of the cluster and $f_0(T)$ has been defined for later use, an explicit version of Eq. (2.10) can be derived. Using the linear approximation for the exponent of Eq. (2.8a),

$$\frac{h_d}{k}\left(\frac{1}{T_0} - \frac{1}{T}\right) \cong \frac{h_d}{kT_0^2}(T-T_0), \tag{2.12}$$

we obtain, upon evaluating the integral in Eq. (2.9),

$$\overline{\gamma_{g+1}(T)} = \gamma_{g+1}^{cl} \exp\left(\frac{h_d^2}{2C_\nu kT_0^2}\right), \tag{2.13}$$

which satisfies Eq. (2.10).

Detailed balance is the statement that for a system at equilibrium the rate of each process, however detailed, is exactly balanced by the rate of the reverse process.[18] In the classical nucleation theory, the fluxes for evaporation and growth at equilibrium are described by the detailed balance condition, Eq. (2.3), with the rate of molecular accommodation by *all g* clusters, in a unit volume, equal to the evaporation rate of *all g*+1 clusters, in the same unit volume, evaluated at the bath temperature T_0. The inequality described by Eq. (2.10) implies a violation of detailed balance since the rate of evaporation, averaged over the cluster distribution, exceeds the rate of molecular accommodation. (See Ref. 10 for a discussion of related violations of the second law.) Equation (2.10) shows that this violation occurs generally and is not a consequence of the Gaussian approximation. Specifically, the rate of cluster evaporation exceeds the rate of condensation by the exponential factor in Eq. (2.13), which is about 1.15 for a 100 molecule cluster, and larger for smaller clusters. The excess evaporation results in a reduced net flux for conversion of g clusters to $g+1$ clusters via (Eq. 2.1). This has a multiplicative effect on the nucleation rate, with a separate factor for each cluster in the sequence from dimer through critical cluster size. The use of $\overline{\gamma_{g+1}(T)}$ in place of γ_{g+1}^{cl} in Eq. (2.3) is the main reason for the prediction of an unphysically large reduction in the nucleation rate.[6,7]

In the following sections we present a theory and an analysis of the problem using a simple stochastic model. There it is shown that the source of the difficulty lies in

application of the conventional expression for the evaporation rate used in classical nucleation theory. Simulation of the evaporation and growth dynamics of *individual* clusters is shown to require a new prescription for handling energy exchange processes. Nevertheless, the conventional treatment is shown to remain valid for describing a canonical *ensemble* of clusters in equilibrium at the temperature of the bath. In other words, the classical theory already averages over the canonical distribution in the derivation of Eqs. (2.4) and (2.8), which are based on Eq. (2.3), so averaging again, as in Eq. (2.9), is superfluous and leads to erroneous results. The development of a general evaporation rate formula, suitable for individual clusters, is presented in Sec. III, which establishes the theoretical foundation for interpretation of the model simulation results presented in Sec. IV.

III. THE EVAPORATION RATE OF SMALL CLUSTERS

This section will begin with an overview of the physics resulting in a simple estimate for the evaporation rate of individual clusters in the capillarity approximation. This is followed by a more general derivation using detailed balance to obtain a formally exact expression for the cluster evaporation rate. The simple estimate, which is adequate for the simulations of Sec. IV, is recovered as a special case of the general rate law when the capillarity approximation is used. Averaging the new evaporation rate law over a canonical distribution of clusters generates the classical nucleation result.

A. An overview of the basic argument

The evaporation rate of a small cluster can be determined from the theory of unimolecular reaction rates applied to the reaction:

$$A_{g+1} \rightarrow A_g + A_1, \tag{3.1}$$

where A_g is a g-molecule cluster and A_1 is a molecule of the vapor phase. The overall decay rate will be proportional to the number of states available to the decay product A_g divided by the number of states available to the reactant A_{g+1} in the energy range dE.[13] This ratio,

$$\frac{w_g(E-h_d)}{w_{g+1}(E)} \cong \frac{\exp[(1/k)S(E-h_d)]}{\exp[(1/k)S(E)]}, \tag{3.2}$$

where E is the total energy of the $g+1$ cluster prior to evaporation, plays the key role in the present analysis of the evaporation rate for small clusters. In writing Eq. (3.2), the Boltzmann relation

$$S(E) = k \ln w(E), \tag{3.3}$$

where $S(E)$ is the entropy of clusters having energy between E and $E+dE$, has been used to obtain the cluster density of states w. The use of the same entropy function in the numerator and denominator of Eq. (3.2) ignores the distinction between clusters of sizes g and $g+1$. This is a good approximation provided that g is not too small. A more complete expression is given in the following section.

In the limit that h_d is small compared to the total energy E, the entropy differences in Eq. (3.2) may be approximated using the entropy derivative

$$\frac{\exp[(1/k)S(E-h_d)]}{\exp[(1/k)S(E)]} \cong \exp\left(\frac{-h_d}{k}\frac{dS}{dE}\right) = \exp\left(\frac{-h_d}{kT}\right), \tag{3.4}$$

where T is the cluster temperature. The last term in Eq. (3.4) gives the T-dependent factor in agreement with Eq. (2.8). Note, however, that the first equality in Eq. (3.4) is only approximate. Specifically, it fails when the energy transferred is an appreciable fraction of E. To address a more general case we invoke the capillarity approximation, assign a temperature to the drop through the mapping $E \leftrightarrow T$, and write the entropy change using the result obtained in the Appendix. [The last term in Eq. (A8) is $-T_0 \Delta S$, where ΔS is the entropy change for the transition from T_0 to T. Here we require the entropy change for the transition from T to $T - h_d/C_\nu$.] Thus, for the exponent in Eq. (3.4), we obtain

$$\frac{1}{k}\left[S(E-h_d) - S(E)\right]$$

$$= \frac{C_\nu}{k} \ln \frac{(T - (h_d/C_\nu))}{T}$$

$$= \frac{C_\nu}{k} \ln\left(1 - \frac{h_d}{C_\nu T}\right)$$

$$= -\frac{h_d}{kT}\left[1 + \frac{1}{2}\left(\frac{h_d}{C_\nu T}\right) + \frac{1}{3}\left(\frac{h_d}{C_\nu T}\right)^2 + \cdots\right] \tag{3.5}$$

showing the correction to the exponent of Eq. (3.4) as an expansion in powers of the fractional energy change (or fractional temperature change) accompanying the transfer of energy h_d.

If we are interested only in the lowest-order correction in Eq. (3.5), we can write an equation similar in structure to Eq. (2.8). First for the entropy change, we obtain

$$\frac{1}{k}\left[S(E-h_d) - S(E)\right] \cong \frac{-h_d}{k(T-\Delta)} \tag{3.6a}$$

with

$$\Delta = \frac{h_d}{2C_\nu}. \tag{3.6b}$$

Equations (3.6) result from comparison of terms through lowest-order correction in Eq. (3.5) with the series expansion for right-hand side of Eq. (3.6a). Comparison with the right-hand side of Eq. (3.4) shows that the lowest-order correction appears as a temperature shift, which is inversely proportional to the cluster size. Then instead of Eq. (2.8), the evaporation rate becomes

$$\gamma^*_{g+1}(T) \cong \gamma^{cl}_{g+1} \exp\left[\frac{h_d}{k}\left(\frac{1}{T_0} - \frac{1}{T-(h_d/2C_\nu)}\right)\right], \tag{3.7}$$

where the asterisk denotes the modified evaporation rate. The approximate equality refers both to use of the capillarity approximation and unfaithful representation of the higher-order terms present in the series expansion of Eq. (3.5). A more complete derivation of Eq. (3.7) is given in Sec. III B based on its deduction from the general result obtained from detailed balance considerations. Note that Eq. (3.7) can be in-
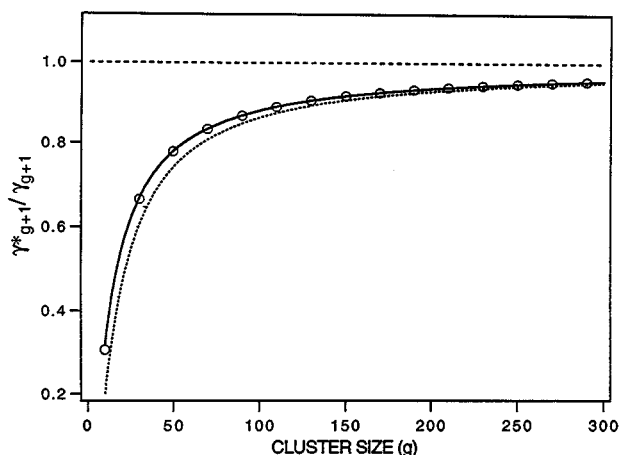
FIG. 1. Evaporation rate as a function of cluster size in the capillarity approximation. Results are for water clusters in the size range $g = 10$–300 molecules at $T = 300$ K. All curves are normalized to the classical ensemble rate expression of Eq. (2.8). Dashed horizontal line, Eq. (2.8); solid curve, modified rate for individual clusters from Eq. (3.7). Circles, result from evaluation of the logarithm in Eq. (3.5) (so as to properly include the higher order terms in the series expansion). The dotted curve results from a similar comparison that neglects the curvature correction to the heat of vaporization from Eq. (2.7) in both the classical and modified rate expressions.

terpreted as assigning an effective evaporation temperature in Eq. (2.8), which is equal to the average of the cluster temperatures before and after evaporation of a monomer has occurred.

A comparison of the evaporation rates from Eqs. (2.8) and (3.7), and from the full series expansion based on Eq. (3.5), is shown for fixed temperature in Fig. 1 as a function of cluster size. It is seen that the ensemble averaging of classical nucleation theory gives large overestimates for the evaporation rates of individual small clusters. In the large-cluster limit, fluctuations in the canonical ensemble become negligible and the two approaches converge to the same result. The figure also shows that Eq. (3.7) is an excellent approximation to the result obtained using the full series expansion of Eq. (3.5) for clusters larger than about 20 molecules. For smaller clusters, other approximations introduced with capillarity drop model begin to fail, including several approximations used in the derivation of Eq. (2.4).[16]

Detailed balance is satisfied when Eq. (3.7) is used in Eq. (2.9) and the integration performed as in Eq. (2.13). Thus, we obtain

$$\overline{\gamma_{g+1}^*(T)} = \int \gamma_{g+1}^*(T) f_0(T) dT = \gamma_{g+1}^{cl} \tag{3.8}$$

for the Gaussian temperature distribution of Eq. (2.11). Unlike Eqs. (2.4) and (2.8), Eq. (3.7) was derived without averaging over an ensemble of clusters. Therefore, it can be applied to individual clusters following the assignment of a temperature to the cluster using the capillarity approximation. That temperature must be a fluctuating quantity on account of the small cluster size and averaging over its distribution is no longer superfluous and, in many applications, may be required. For example, to make contact with classical nucleation theory we must average the modified rate over the canonical ensemble. Equation (3.8) shows that the averaged rate satisfies detailed balance and agrees with the rate from classical nucleation theory. Equation (3.7) will be tested further in the simulations of Sec. IV.

B. Detailed balance

The detailed balance condition, Eq. (2.3), can also be used to derive the differential evaporation rate, which we define as the rate of evaporation when the cluster energy is in the range E to $E + dE$. Considering only that subset of $g+1$ clusters whose energy lies in this range, Eq. (2.3) becomes

$$\beta_1 s_g n_g(E - h_d) = \gamma_{g+1}^*(E) s_{g+1} n_{g+1}(E). \tag{3.9}$$

Solving for the differential evaporation rate we obtain

$$\gamma_{g+1}^*(E) = \beta_1 \frac{s_g n_g}{s_{g+1} n_{g+1}} \left(\frac{n_g(E - h_d)/n_g}{n_{g+1}(E)/n_{g+1}} \right)$$

$$= \gamma_{g+1} \frac{n_g(E - h_d)/n_g}{n_{g+1}(E)/n_{g+1}}, \tag{3.10}$$

where γ_{g+1} is from Eq. (2.3). Like γ_{g+1}^{cl}, which results *after* invoking the capillarity approximation, γ_{g+1} is applied only at the temperature of the bath. Noting that the denominator in Eq. (3.10) gives the probability for a $g+1$ cluster to have energy in the range E to $E + dE$, it is easily shown that Eq. (3.10) satisfies detailed balance after integration over the cluster energy distribution. Thus,

$$\overline{\gamma_{g+1}^*(E)} = \int \gamma_{g+1}^*(E) P(E) dE$$

$$= \gamma_{g+1} \int \left(\frac{n_g(E - h_d)/n_g}{n_{g+1}(E)/n_{g+1}} \right) \frac{n_{g+1}(E)}{n_{g+1}} dE$$

$$= \gamma_{g+1} \int \left(\frac{n_g(E - h_d)}{n_g} \right) dE = \gamma_{g+1}. \tag{3.11}$$

To evaluate the cluster distributions appearing in Eq. (3.10), it is convenient to use the grand ensemble. Summing over all states in the energy range E to $E + dE$, and using Eq. (3.3) gives

$$\frac{n_g(E - h_d)}{n_{g+1}(E)} = \frac{\exp[(1/k)S_g(E - h_d)]\exp[-(E - h_d)/kT_0]\exp(g\mu_\nu/kT_0)}{\exp[(1/k)S_{g+1}(E)]\exp(-E/kT_0)\exp[(g+1)\mu_\nu/kT_0]}. \tag{3.12a}$$

Furthermore,

$$\frac{n_{g+1}}{n_g} = \frac{q_{g+1}\exp[(g+1)\mu_\nu/kT_0]}{q_g\exp[g\mu_\nu/kT_0]} = \frac{q_{g+1}}{q_g}\exp\left(\frac{\mu_\nu}{kT_0}\right), \tag{3.12b}$$

where μ_ν is the molecular chemical potential of the vapor and q_g is the canonical partition function for a stationary cluster of size g. Substitution of Eqs. (3.12) into Eq. (3.10) gives

$$\gamma^*_{g+1}(E) = \gamma_{g+1} \frac{q_{g+1} \exp[(1/k)S_g(E-h_d)]\exp(h_d/kT_0)}{q_g \exp[(1/k)S_{g+1}(E)]},$$
(3.13)

showing the required independence of the evaporation rate on μ_ν. Equation (3.13) is a formally exact expression for the evaporation rate of a cluster of energy E.

The capillarity approximation can be used to evaluate the right hand side of Eq. (3.13). Thus, for example,[16]

$$-kT_0 \ln q_g = g\mu_l + \sigma s_g,$$
(3.14)

where μ_l is the chemical potential of the bulk liquid and the remaining quantities are as previously defined. Equations (3.12b) and (3.14) give the ratio of equilibrium cluster populations, at the temperature of the bath, in agreement with Eq. (2.4). For cluster sizes that are not too small, e.g., $g > 20$, it is a good approximation to neglect the distinction between clusters of sizes g and $g+1$ in Eq. (3.13) to obtain

$$\gamma^*_{g+1}(E) \cong \gamma_{g+1} \exp\left\{ \frac{1}{k} \left[S(E-h_d) - S(E) \right] \right\} \exp\left(\frac{h_d}{kT_0} \right)$$

$$= \gamma_{g+1} \exp\left\{ -\frac{1}{kT_0} \left[W(E-h_d) - W(E) \right] \right\}, \quad (3.15)$$

where W is the Helmholtz free energy.

As in Eq. (3.11), it is readily found that the differential evaporation rate defined by Eq. (3.15) satisfies detailed balance after averaging over the cluster energy distribution. The distribution function for equilibrium fluctuations in the energy is given by Eq. (A11) thus

$$P(E) = K \exp\left(-\frac{W(E)}{kT_0} \right),$$
(3.16)

where K is the normalization constant for the energy distribution. Carrying out the integration, as in Eq. (3.11), we obtain

$$\overline{\gamma^*_{g+1}(E)} = \gamma_{g+1} K \int_{h_d}^{\infty} \exp\left\{ -\frac{1}{kT_0} \left[W(E-h_d) \right.\right.$$

$$\left.\left. - W(E) \right] \right\} \exp\left(-\frac{W(E)}{kT_0} \right) dE$$

$$= \gamma_{g+1} K \int_{h_d}^{\infty} \exp\left(-\frac{W(E-h_d)}{kT_0} \right) dE$$

$$= \gamma_{g+1} K \int_{0}^{\infty} \exp\left(-\frac{W(E)}{kT_0} \right) dE$$

$$= \gamma_{g+1}.$$
(3.17)

The lower limit in the first two integrals is set by the requirement of positive energy and the last integral uses the variable substitution $E = E - h_d$.

Equation (3.7) is recovered as a special case of the general rate law when the capillarity approximation is used. Re-

turning to Eq. (3.15), we note that the entropy factor is identical to the right-hand side of Eq. (3.2). Using either Eqs. (3.5) or (3.6) for the entropy differences and making the replacements, γ^{cl}_{g+1} for γ_{g+1} and T for E, gives the modified evaporation rate in terms of the cluster temperature T. Specifically, the use of Eq. (3.6) for the entropy difference gives immediate recovery of Eq. (3.7). The latter, in turn, approaches the classical ensemble rate of Eq. (2.8) when the fractional energy exchange is small (Fig. 1).

IV. A STOCHASTIC MODEL FOR FLUCTUATIONS DURING EVAPORATION AND GROWTH

In this section we develop a direct approach to temperature fluctuations via the simulation of a specific coupling channel between the cluster and the bath. The bath consists of a large nondepletable reservoir of vapor at fixed temperature and pressure. The coupling to the bath is through the evaporation and condensation of vapor molecules. The essential features of the capillarity approximation used in the simulation are the following. (1) Its mapping of physical clusters into spherical drops having bulk thermodynamic properties including well-defined values for surface tension, temperature, heat capacity, etc. (2) Fluctuations in drop size, energy, and temperature are included through direct simulations that incorporate the fundamental statistical character of evaporation and growth processes while neglecting the details of molecular interaction.

A. Description of the model for a single coupling channel

To focus the present analysis, we limit the model to a single coupling channel, or mode of energy exchange, between the cluster and the bath. Thus we neglect in the simulations, but not in the qualitative discussion, the effects of collisional and radiative energy transfer. Radiative transfer has a negligible effect under conditions similar to those of the present calculations (2), but the stochastic model can be used to include radiative transfer for other applications (Sec. V). Energy transfer through collisions with background gas and/or noncondensing vapor species has important implications for the model and will be discussed. For example, it will be shown that the modified evaporation rate for small clusters results in a distribution of fluctuations in temperature or energy that is invariant to the fraction of energy dissipated through nonaccommodating collisions, while for the unmodified evaporation rate [Eq. (2.8)] this is not the case.

The major advantage of working with the single channel model is that a single component cluster is constrained to be in stable equilibrium with its environment and good statistics can be obtained without drift in cluster energy or size. Each condensation step increases the energy of the cluster by an amount equal to the latent heat. This, in turn increases the evaporation rate and, therefore, the rate of energy removal. Similarly, each evaporation step decreases both the cluster energy and evaporation rate, and, therefore, enhances the relative probability that the next event will be a condensation step. Consequently, in this model the cluster is stable, fluctuations regress, and T is a function of the cluster size:

$$T = T_0 + \frac{h_d}{C_\nu}(g - g_0). \qquad (4.1)$$

Here g_0 is the initial cluster size at the temperature T_0 of the bath.

Rules for updating the simulation model are as follows: Both growth and evaporation are modeled as Poisson distributed processes by maintaining the computational time step (τ) sufficiently small that the occurrence of either multiple growth or multiple evaporation events, within any single time step, is a rare event. The growth sequence is simulated using Poisson arrival times for monomer at a fixed mean rate (per unit area of cluster surface) determined by the molecular accommodation frequency through Eq. (2.2). A vapor accommodation coefficient of unity is assumed. The evaporation sequence is also simulated using Poisson statistics, but here the unit area departure rate varies depending on the temperature of the drop. We will investigate both Eqs. (2.8) and (3.7) for determining the temperature dependence of the evaporation rate. Finally, the energy and temperature of the drop are updated after each growth or evaporation event. Each condensing molecule adds h_d to the energy of the cluster and h_d/C_ν to its temperature, while each evaporating molecule removes these amounts. Diffusion of heat within the cluster is assumed to be sufficiently rapid, relative to the time interval between successive growth/evaporation events, that the temperature within the cluster is uniform. This completes the rules for implementing the single-channel stochastic model.

B. Simulation results

Calculations are presented here for water clusters in the 50–300 molecule size range. These clusters are sufficiently large that fractional changes in size can be neglected, but small enough to be in a range where the studied effects can be easily seen. For a cluster size of 11 molecules at $T_0 = 300$ K, $\Delta T/T \cong 0.1$, where ΔT is the standard deviation of the temperature fluctuation [Eq. (A14)]. For a cluster size of thirteen molecules we find $\Delta S/S \cong 0.1$ for fluctuations in entropy, taking the bulk liquid entropy value at this temperature from Ref. 19 for the capillary drop. Thus the relative temperature and entropy fluctuations of the simulated clusters are less than those encountered in statistical models of the nucleus where the temperature concept has been employed.[11]

Poisson statistics is achieved by setting τ equal to 1/40 of the average time between collisions of the vapor with the cluster surface. Simulation results were found to be independent of this setting for values of τ below about 1/10 of the average collision time. Separate random number sequences, generated using the program RAN2,[20] are used to decide whether an evaporation or growth event takes place within each successive time step of the simulation. Bulk liquid water properties required in the capillarity approximation are from Ref. 19. Equilibrium is achieved by setting the vapor pressure used to compute the molecular accommodation rate, via Eq. (2.2), equal to the vapor pressure of the drop. The latter follows the Kelvin relation
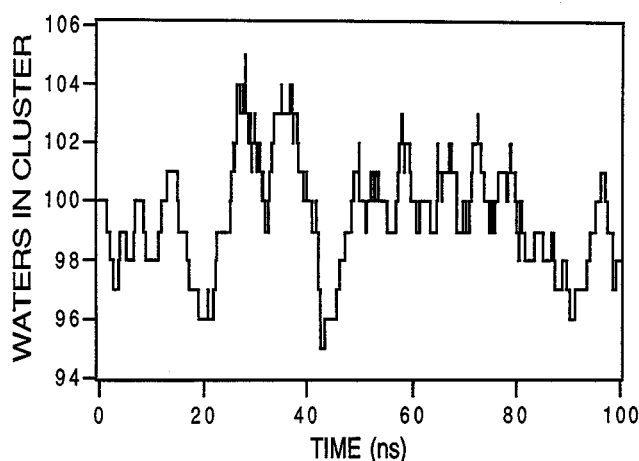
FIG. 2. Fluctuations in cluster size versus time. Results obtained from the stochastic condensation/evaporation simulation model for an initial cluster of 100 molecules in equilibrium at a bath temperature of 300 K.

$$p_1 = p_1(r_g, T_0) = p_1(\infty, T_0)\exp\left(\frac{2\sigma}{r_g k T_0}\nu_1\right) \qquad (4.2)$$

evaluated at $g = g_0$. Equations (2.4) and (2.8b) determine the classical evaporation rate γ_{g+1}^{cl}, which is the prefactor in Eqs. (2.8) and (3.7).

Figures 2 and 3 show statistically independent time sequences for temperature and number of molecules, respectively, in a drop undergoing evaporation and growth. Initial conditions are a cluster size of 100 molecules in equilibrium at the bath temperature, 300 K. The regression of fluctuations that results from cluster stability is clearly evident in the figures, as are the quantized jumps in number and temperature, corresponding to integer values of g in Eq. (4.1). Accurate estimates of the fluctuation variance, and quantitative tests of the different expressions for the evaporation rate, Eqs. (2.8a) and (3.7), require a level of statistical resolution that can only be achieved when much longer time sequences are examined. These results are reported in Figs. 4–6.
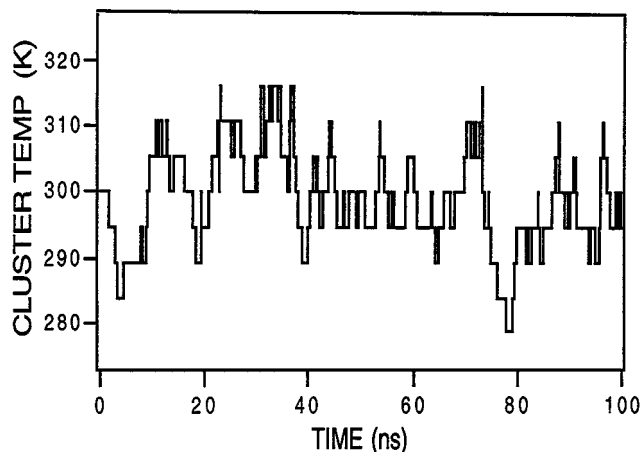
FIG. 3. Fluctuations in cluster temperature versus time. Conditions are the same as in Fig. 2. The fluctuations are uncorrelated with those shown in Fig. 2 due to the use of a different random number generator seed.
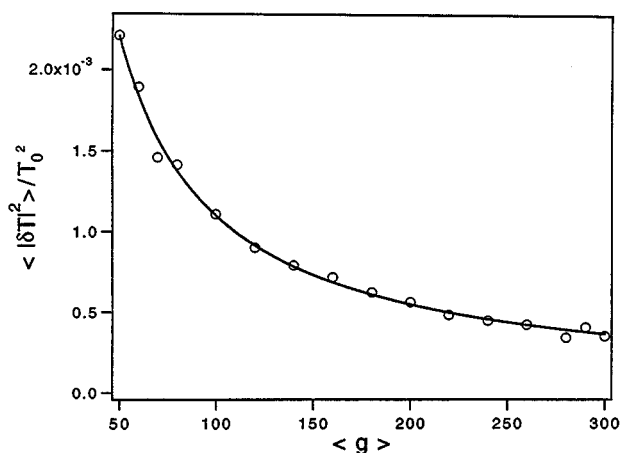
FIG. 4. Temperature fluctuations versus cluster size. The smooth curve is k/C_ν, the circles are the simulation results. Each circle represents a time sequence of approximately 5000 random evaporation/condensation steps observed over a period of 200 000 computational steps.

Figure 4 shows the mean-square temperature fluctuation as a function of the average cluster size. (For any given simulation run, there is essentially no difference between the average and initial cluster size on the scale of the figure, so we approximate the average cluster size by the initial size, g_0.) The observed fluctuation variance is seen to follow the standard theoretical relation (Appendix):

$$\langle|\delta T|^2\rangle = kT_0^2/C_\nu. \tag{4.3}$$

Each circle represents the statistics garnered from a time sequence of approximately 5000 random evaporation/condensation events observed over a period of 200 000 computational time steps. (This is on the order of 10 μs in real time for the 50 molecule cluster, which is well beyond the range of full molecular dynamics simulation.) The fluctuation variance is not particularly sensitive as to whether Eq.
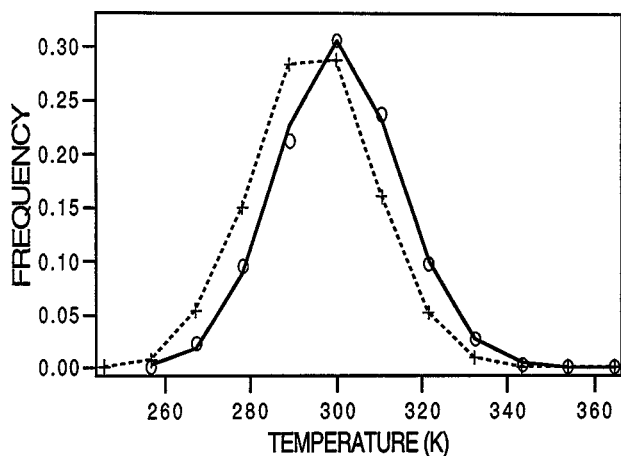
FIG. 5. Temperature fluctuation distributions for an initial cluster size of 50 molecules. Crosses result when the classical expression for the evaporation rate [Eq. (2.8)] is applied to the simulated cluster. Circles result using the corrected evaporation rate law [Eq. (3.7)]. The solid line is the theoretical result derived in the Appendix [Eqs. (A8) and (A9)].
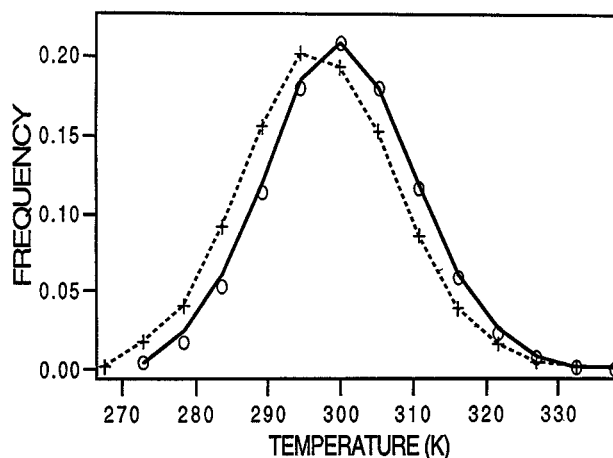
FIG. 6. Same as in Fig. 5 except for an initial cluster size of 100 molecules.

(2.8) or (3.7) is used. Figure 4 was obtained using the modified evaporation rate, Eq. (3.7), which gives excellent agreement with the theoretical curve. [A slight, systematically positive, deviation from the theoretical curve was observed when Eq. (2.8) was used.]

More interesting are the temperature distributions themselves. These are shown in Fig. 5 for an initial cluster size of 50 molecules and bath temperature equal to 300 K. The crosses, joined by the dashed line segments, result using Eq. (2.8) for the evaporation rate. Here we show the normalized distribution resulting after 200 000 computational time steps (again approximately 5000 random evaporation/condensation events). Note that the average temperature appears to be shifted by the amount Δ from Eq. (3.6b), equal to about 1/2 the point spacing seen in the figure, *below* the temperature of the bath. The circles result from a similar calculation using the modified evaporation rate [Eq. (3.7)]. The solid line segments connect points obtained from the theoretical fluctuation distribution [Eqs. (A8) and (A9)] evaluated at temperatures corresponding to integer values of g in Eq. (4.1). Figure 6 shows similar results for a 100 molecule cluster, but with less prominent differences between the corrected and uncorrected distributions, as expected from a doubling of C_ν.

Several comments can be made about these distributions. First, all of the simulated distributions satisfy detailed balance for the corresponding evaporation rate. The distributions resulting from Eq. (2.8) satisfy detailed balance at the expense of an unphysical shift to temperatures below the temperature of the bath. The distributions of Figs. 5 and 6 are non-Gaussian. However, the cluster sizes are not so small that they are far from the Gaussian limit and it is instructive to examine this case. Then the theoretical distribution for fluctuations in temperature follows $f_0(T)$, defined in Eq. (2.11), and it is readily shown that the following integral identities hold: First, using the modified evaporation rate,

$$\overline{\gamma_{g+1}^*(T)} = \int \gamma_{g+1}^*(T)f_0(T)dT = \gamma_{g+1}^{cl}, \tag{4.4}$$

where γ^* is from Eq. 3.7 [this is Eq. (3.8)]. Shifting the variable of integration we obtain

$$\overline{\gamma^*_{g+1}(T)} = \int \gamma^*_{g+1}(T+\Delta)f_0(T+\Delta)dT$$

$$= \int \gamma_{g+1}(T)f_0(T+\Delta)dT = \gamma^{\rm cl}_{g+1}, \qquad (4.5)$$

where in the last equality γ is from Eq. (2.8), but the temperature distribution has been shifted to lower temperatures by the amount

$$\Delta = \frac{h_d}{2C_\nu}$$

from Eq. (3.6b). Equations (4.4) and (4.5) give an excellent description of the effects seen in Figs. 5 and 6. In particular, the last equality of Eq. (4.5) supports the shifted temperature distributions shown by the dashed curves in Figs. 5 and 6.

C. A qualitative description of the effects of a background gas

When the conventional evaporation rate expression, Eq. (2.8), is applied to individual clusters, as in the dashed curves of Figs. 5 and 6, the time-average cluster temperature is shifted below the temperature of the bath. In this case energy transfer by collisions with a noncondensable background gas will tend to restore the cluster temperature to that of the bath, favoring increased evaporation and, therefore, a reduction in the nucleation rate. In the high pressure limit we would expect the distribution to center on the bath temperature and Eq. (2.13) would imply extreme reductions in the nucleation rate, following the discussion presented in Sec. II. Such effects are not supported by recent experiments, which indicate little or no influence of background gas pressure on nucleation rate.[21–23] Even more seriously, one can deduce, from the situation just described, the existence of a cyclic process at equilibrium with a step that includes unidirectional net energy transfer from the background gas to the cluster—in violation of detailed balance.[24]

From the preceding analysis we conclude that while Eq. (2.8) can be made to satisfy detailed balance in the absence of collisional energy transfer, it cannot be a valid expression for describing energy transfer processes involving single small clusters, or groups of small clusters where averaging over the canonical distribution is incomplete. For this purpose Eqs. (3.7) or (3.13) should be used. Then the distribution of cluster energy at equilibrium (over time) will correctly satisfy the canonical Boltzmann distribution law, and be invariant to the specific nature of the coupling channel(s) between the cluster and the bath. Thus, for systems in stable equilibrium, inclusion of a background gas will have no significant effect on cluster fluctuations or on maintenance of the detailed balance condition. (At extreme gas pressures there will be a vapor pressure increase but this effect is generally not included in the classical theory.) Thus Eqs. (3.7) or (3.13) can be used, whether or not additional coupling channels are included in the model. Similarly, h_d has until now referred specifically to the energy exchange accompanying an evaporation or condensation event. The analysis of Sec. III is not limited to this case and should be applied even when h_d represents a quantity of energy transferred by other mechanisms, including collisional energy transfer, that couple the system to the bath. If g doesn't change during the transfer, Eq. (3.15) can be used.

V. SUMMARY AND DISCUSSION

In this paper we have shown that although fluctuations in cluster energy and temperature are not included explicitly in the classical nucleation theory, which considers all clusters in equilibrium at the bath temperature, they are properly accounted for through the equilibrium assumption implicit in the detailed balance condition, Eq. (2.3). Consequently, the classical expression for the evaporation rate that appears in Eqs. (2.3), (2.4), and (2.8) must be interpreted as applying to an ensemble of clusters in equilibrium at the temperature of the bath. Difficulties, in the form of detailed balance violation, arise when the attempt is made to apply this form to individual clusters. Nevertheless, the need to determine the evaporation rates for individual clusters (or groups of clusters having the same energy) is evident. Examples include studies of individual clusters, as presented in Sec. IV, and nonisothermal nucleation processes where there is a need to track fluxes in both cluster energy and cluster size. In these cases it is meaningless to first average over energy, so the use of Eq. (2.8), e.g., which implies such an average, is not appropriate and can lead to erroneous results.

Simulation of the evaporation and growth dynamics of individual clusters has been shown to require a new prescription for handling energy exchange processes that results in a different evaporation rate law from that encountered in classical nucleation theory. Only in the limit that the energy of exchange is a small faction of the total available cluster energy are the two forms equivalent. A major result of the present study has been the development of a formally exact expression for the single-cluster evaporation rate [Eq. (3.13)]. The approximate evaluation of this expression in Sec. III is a new application of the capillarity approximation, namely, its use to determine the evaporation rate of small clusters without ensemble averaging. The new rate law reduces to Eq. (3.7) for ready evaluation and testing in the simulation model. The single-cluster rate expressions enable one to recover the classical nucleation result for a canonical ensemble of clusters by averaging over the distribution—the detailed balance condition is always satisfied. Thus we may replace the classical evaporation term in Eq. (2.3) (γ_{g+1}) with the explicit averaged value ($\overline{\gamma^*_{g+1}}$) since these are equal for the modified cluster evaporation rate as shown by Eqs. (3.11) and (3.17), or by Eq. (3.8) in the capillarity approximation.

The second result of this paper has been the development of a stochastic simulation model for describing cluster evaporation and growth statistics in the capillary approximation. Despite its current application to a single coupling channel, the model is successful in resolving differences between the evaporation rates given by Eqs. (2.8) and (3.7) and in reproducing the fluctuation spectrum, as derived from the

Einstein fluctuation formula in the Appendix, when the modified rate from Eq. (3.7) is used.

With further development, the stochastic model will likely prove advantageous for extension to multicomponent systems with multiple coupling channels. For multicomponent systems, it is well known that stable equilibria between a drop and its vapor can occur. Indeed, this stability plays a major role in determining the optical properties of atmospheric aerosols and activation processes in clouds. Consider, for example, a two-component drop consisting of a nonvolatile solute in water. This drop coexists in equilibrium with water vapor along the stable branch of the Kohler curve that describes the size of the drop as a function of relative humidity.[25] Another example, although not a case of true stability, is provided by sulfuric acid-water clusters in binary nucleation.[26,27] Here the exchange of water vapor is fast compared with exchange of sulfuric acid, which is generally present in only trace amounts. As a result, clusters are in local equilibrium with respect to evaporation and condensation of water vapor. Recent work suggests that fluctuations become large at boundaries between stable and unstable branches of the Kohler curve.[27] The stochastic model should provide an ideal tool for simulating such fluctuations. With further extension, which will likely include some coarse graining of the fluctuations, the model should prove useful for statistical simulations of heterogeneous nucleation processes in clouds. These systems will be the subject of future studies.

A final interesting consequence of the simulation model is seen in Fig. 4. Here the model successfully predicts the variance of the temperature fluctuation given only the assumption of Poisson statistics and the Clapeyron temperature dependence of the evaporation rate. This result implies a fundamental connection between Eq. (4.3) for the fluctuations, Poisson statistics for the arrival and departure of molecules, and the Clapeyron temperature dependence of Eqs. (2.8) and (3.7). As a further test of the model, similar calculations were carried out for radiative transfer with absorption and emission of photons serving as the coupling channel between the particle and the bath. Equation (4.3) for the fluctuations was again found to be satisfied. However, the rates of photon emission from the particle were found to be consistent with the Wien distribution law—the high frequency form of the Planck distribution. [The Wien law gives a temperature-dependent photon emission rate similar to Eq. (2.6), except that the photon energy $h\nu$ appears in place of h_d on the right-hand side.] This result was determined to be a consequence of the assumption of Poisson statistics, which for photons is valid only in the shot limit $h\nu \gg kT$.

During this work it was brought to our attention that several authors have suggested a modification to the classical nucleation kinetics [Eq. (2.1)] by noting that when molecules condense on a curved surface, the area available for condensation is not the area of the surface itself, but the larger exterior area of an added outer shell of thickness equal to the molecular radius.[28,29] This correction will not effect the ratio of the modified to classical expressions for the evaporation rate (Fig. 1), which results from the theory presented here, but it may have an effect on the classical rate itself. How-

ever, since the correction is purely kinetic, the equilibrium cluster populations will be unchanged and any effect on the unit-area evaporation rate of Eq. (2.4) must be small. How small it is will depend on how one applies the correction to the surface area available for evaporation. If the added-shell structure, shown in Fig. 1 of Ref. 29, is interpreted as a transition state for the reaction described by Eq. (3.1), then it seems natural to replace the ratio s_g/s_{g+1} by unity in the first equality of Eq. (2.4) to correct the evaporation rate. For a 50-molecule cluster, this is on the order of a 1% change. The stochastic model simulations will be affected by the increased condensation/evaporation rates that result from augmenting the surface area factors in Eq. (2.1). Mainly there will be a slight compression of the fluctuation time scale of Figs. 2 and 3 (by about 20%) due to the faster rates for evaporation and growth. The fluctuation distribution results shown in Figs. 4–6 will be unchanged.

ACKNOWLEDGMENTS

APPENDIX: THE DISTRIBUTION OF TEMPERATURE AND ENERGY FLUCTUATIONS FOR SMALL SYSTEMS COUPLED TO A HEAT BATH

In this Appendix we first calculate the reversible work required to change the temperature of a small system from that of the bath to which it is coupled. The Einstein relation (15), connecting the probability of a fluctuation in a variable x with the reversible work required to produce that fluctuation through the application of external constraints, is then used to obtain the probability distribution function for fluctuations, where x is either the temperature or energy of the system. We will focus on the temperature fluctuation distribution to obtain the theoretical curves shown in Figs. 5 and 6. The energy fluctuation can be obtained from the temperature fluctuations using $dE = C_v dT$.

To derive the reversible work we imagine a Carnot engine providing the coupling between the system and the bath as depicted in Fig. 7. This is used to bring the system to a temperature T, which can be either less than or greater than the bath temperature T_0. For the case that T is less than T_0 (case 1 of Fig. 7) the condition of reversibility requires

$$\Delta S = -\frac{Q_1}{T} + \frac{Q_2}{T_0} = 0. \tag{A1}$$

Combining this result with the first law

$$Q_1 + W = Q_2, \tag{A2}$$
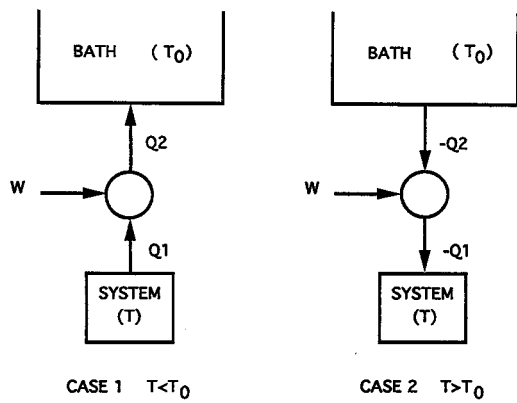
FIG. 7. Carnot engine coupling of a small system to a heat bath.

gives the usual result for the Carnot efficiency

$$\eta^- \equiv \frac{W}{Q_1} = \frac{T_0 - T}{T}, \tag{A3}$$

where the superscript $(-)$ signifies the cooling case ($T<T_0$, $dT<0$). Applying this last result to differential changes in the heat and work gives

$$dQ_1 = \frac{T}{T_0 - T} dW = -C_\nu dT. \tag{A4}$$

A similar analysis for heating ($T>T_0$ and $dT>0$) corresponding to case 2 of Fig. 7 yields

$$\eta^+ \equiv \frac{W}{-Q_1} = \frac{T - T_0}{T} \tag{A5}$$

and

$$-dQ_1 = \frac{T}{T - T_0} dW = C_\nu dT \tag{A6}$$

in place of Eqs. (A3) and (A4), respectively. Thus, in either case, heating [Eq. (A6)] or cooling [Eq. (A4)], we have

$$dW = -C_\nu \left(\frac{T_0 - T}{T} \right) dT. \tag{A7}$$

The reversible work is obtained by integrating Eq. (A7) from T_0 to T to obtain

$$W(T) = \int_{T_0}^{T} -C_\nu (T_0 - T)/T \ dT$$

$$= C_\nu (T - T_0) + C_\nu T_0 \ln(T_0/T), \tag{A8}$$

which is equal to the Helmholtz free-energy change.

The Einstein relation (15) gives the temperature fluctuation distribution as

$$P(T) = K_1 \exp[-W(T)/kT_0], \tag{A9}$$

where K_1 is a normalization constant. Equation (A9), with $W(T)$ from Eq. (A8), was used to obtain the theoretical distribution curves shown in Figs. 5 and 6. The distribution has the property that the average value of the reciprocal temperature equals the reciprocal of the bath temperature. Thus,

$$\left\langle \frac{1}{T} \right\rangle = K_1 \int_0^\infty \frac{1}{T} \exp[-W(T)/kT_0] dT$$

$$= K_1 \int_0^\infty \left(-\frac{1}{C_\nu T_0} \frac{dW}{dT} + \frac{1}{T} \right) \exp[-W(T)/kT_0] dT$$

$$= \frac{-K_1}{C_\nu T_0} \int_0^\infty \frac{dW}{dT} \exp(-W/kT_0) dT + \frac{K_1}{T_0}$$

$$\times \int_0^\infty \exp(-W/kT_0) dT$$

$$= \frac{-K_1}{C_\nu T_0} \int_{W(0)}^{W(\infty)} \exp(-W/kT_0) dW + \frac{1}{T_0}$$

$$= \frac{1}{T_0}, \tag{A10}$$

which is a special case of a more general identity established in Ref. 10.

The distribution of energy fluctuations in the canonical ensemble follows the Boltzmann form[10]

$$P(E) = K_2 \exp\left(\frac{S(E)}{k} \right) \exp\left(-\frac{E}{kT_0} \right)$$

$$= K_2 \exp\left(-\frac{W(E)}{kT_0} \right), \tag{A11}$$

where K_2 is the normalization constant, the density of states has been written in terms of the entropy, as in Eqs. (3.2) and (3.3), and the definition of the Helmholtz free energy ($W = E - T_0 S$) has been used. Note that Eq. (A11) is a general expression that does not require the capillarity approximation.

For large clusters, C_ν is large and the distribution of fluctuations is sharply peaked about the bath temperature T_0. It is useful to consider the first-order approximation to $P(T)$ valid when the fluctuations about the bath temperature are small compared to the bath temperature itself. Then expansion of the logarithm in Eq. (A8) and noting the cancellation of the linear terms gives

$$W(T) \cong \frac{1}{2} \frac{C_\nu}{T_0} (T - T_0)^2, \tag{A12}$$

where the approximate equality signifies the neglect of higher terms from the expansion. Substitution into Eq. (A9) yields a Gaussian approximation for the distribution $P(T)$:

$$P(T) \cong \left(\frac{C_\nu}{2\pi k T_0^2} \right)^{1/2} \exp\left[\frac{-C_\nu (T - T_0)^2}{2k T_0^2} \right] \tag{A13}$$

which is valid for $|T - T_0|/T_0 \ll 1$. Equation (A13) results in the standard expressions for the mean-square fluctuations (variance) in temperature and energy:

$$\langle |\delta T|^2 \rangle = k T_0^2 / C_\nu,$$

$$\langle |\delta E|^2 \rangle = k T_0^2 C_\nu. \tag{A14}$$

For larger (non-Gaussian) fluctuations Eqs. (A8) and (A9) should be used.

[1] F. F. Abraham, *Homogeneous Nucleation Theory* (Academic, New York, 1974), p. 82.

[2] B. E. Wyslouzil and J. H. Seinfeld, J. Chem. Phys. **97**, 2661 (1992).

[3] A. Kantrowitz, J. Chem. Phys. **19**, 1097 (1951).

[4] R. F. Probstein, J. Chem. Phys. **19**, 619 (1951).

[5] J. Feder, K. C. Russell, J. Lothe, and G. M. Pound, Adv. Phys. **5**, 111 (1966).

[6] I. J. Ford and C. F. Clement, J. Phys. A **22**, 4007 (1989).

[7] C. F. Clement and I. J. Ford, J. Aerosol Sci. **20**, 1015 (1989).

[8] J. C. Barrett, C. F. Clement, and I. J. Ford, J. Phys. A **26**, 529 (1993).

[9] R. McGraw and R. A. LaViolette, in *Proceedings of the 64th Colloid and Surface Science Symposium and Nucleation Symposium*, Lehigh University, June 18–20, 1990, p. 25.

[10] R. McFee, Am. J. Phys. **41**, 230 (1973).

[11] H. Feshbach, *Phys. Today* 9 (Nov. 1987).

[12] C. Kittel, *Phys. Today* 93 (May 1988).

[13] V. F. Weisskopf, Phys. Rev. **52**, 295 (1937).

[14] J. M. Blatt and V. F. Weisskopf, *Theoretical Nuclear Physics* (Wiley, New York, 1952), p. 369.

[15] R. C. Tolman, *The Principles of Statistical Mechanics* (Dover, New York, 1979), p. 638.

[16] C. L. Weakliem and H. Reiss, J. Phys. Chem. **98**, 6408 (1994).

[17] W. Feller, *An Introduction to Probability Theory and its Applications* (Wiley, New York, 1971), Vol. 2, p. 153.

[18] R. D. Levine and R. B. Bernstein, *Molecular Reaction Dynamics and Chemical Reactivity* (Oxford, New York, 1987), Chap. 4.

[19] D. Eisenberg and W. Kauzmann, *The Structure and Properties of Water* (Oxford, New York, 1969).

[20] W. H. Press, W. T. Vetterling, S. A. Teukolsky, and B. P. Flannery, *Numerical Recipes in* FORTRAN (Cambridge, New York, 1992).

[21] P. E. Wagner, R. Strey, and Y. Viisanen, in *Nucleation and Atmospheric Aerosols*, edited by N. Fukuta and P. E. Wagner (Deepak, Hampton, Virginia, 1992), pp. 27–29.

[22] M. P. Anisimov and S. N. Vershinin, J. Aerosol. Sci. **21**, S11 (1990); **21**, S15 (1990).

[23] B. E. Wyslouzil, G. Wilemski, M. G. Beals, and M. B. Frish, Phys. Fluids **6**, 2845 (1994).

[24] L. Onsager, Phys. Rev. **37**, 405 (1931).

[25] H. R. Pruppacher and J. D. Klett, *Microphysics of Clouds and Precipitation* (Reidel, Dordrecht, 1980), Chap. 6.

[26] R. McGraw, J. Chem. Phys. **102**, 2098 (1995).

[27] H. Reiss and G. J. M. Koper, J. Phys. Chem. (to be published).

[28] L. Dufour and R. Defay, *Thermodynamics of Clouds* (Academic, New York, 1963), Chap. 13.

[29] F. G. Shi, Scr. Meta. Mater. **30**, 1195 (1994).